Journal of Space Operations & Communicator (ISSN 2410-0005)
Vol. 16, No. 1, Year 2019

The Local Coverage Diagram, A Tool for Satellite Orbit Analysis

E. F. M. Jochim[1], Th. Neff[2], B. Calaminus[3]
German Aerospace Center (DLR), Oberpfaffenhofen, Germany

With the local coverage diagram a tool for a longterm survey on frequency and quality of contacts of a near Earth satellite with a point of interest on the Earth's surface is realized. It respects different coverage or visibility conditions of a satellite with its ground station. Special interest is based on characterising coverage patterns for different satellite families like near Earth missions, repetitive and/or sunsynchronous orbits, orbits with required local time shift per draconic period, satellite orbits with manoeuvre or uncontrolled satellite orbits as well as for satellite constellations. The tool allows an easy detection of observation of different satellite orbits with observation conflicts. The local coverage pattern is of interest for orbit analysis investigations, for operational use in satellite ground centres as well as for educational purposes.

Nomenclature

a	=	semimajor axis [km]
e	=	eccentricity
H	=	height [km] of satellite with respect to mean equatorial radius
h	=	height ("elevation") [degree]
i	=	inclination [degree]
K	=	characteristic for coverage quality
$n_{\odot}$	=	mean tropical motion of apparent Sun [rad/s]
W	=	swath width [km]
z	=	zenith distance [degree] ("angle of incidence")
β	=	(off) nadir angle [degree]
γ	=	central angle [degree]
λ	=	geographic longitude (positive towards east) [degree]
φ	=	geodetic latitude [degree]
$\dot{\Omega}_s$	=	secular drift of node [degree/day, or: rad/s]

1. Basics for the Local Coverage Investigations

In order to support the satellite during orbit injection so-called visibility diagrams were developed in the years 1972-1979. With different resolutions a detailed contact analysis between satellite, interplanetary space probes, planetary and stellar objects with ground stations at the Earth's surface or above (airplanes, sounding rockets etc.) was presented ([3], [4], [5], [6]).

[1] Dr. Ing., retired scientific coworker, DLR Microwaves and Radar Institute (fritz.jochim@dlr.de)
[2] Dr. Ing., Head of Reconnaissance and Security Department, DLR Microwaves and Radar Institute, Oberpfaffenhofen, 82234 Weßling, Germany
[3] Dipl. Ing., M.Sc., scientific coworker, formerly DLR Microwaves and Radar Institute

In the present study however, a plot diagram will be proposed preparing a longterm overview how often and in which quality a certain target point or a selected scene on the Earth's surface or a ground station will be covered by a certain type of sensor onboard a satellite. The diagram reflects each pass of a satellite with respect to the target point fulfilling required observability conditions. The original presentation with figures was replaced by a new graphic software [1] allowing a fast overview about the contact qualities versus time as well as interactions between interfering observations with different satellites at the same time. A first version of the new tool was presented in 2008 [9].

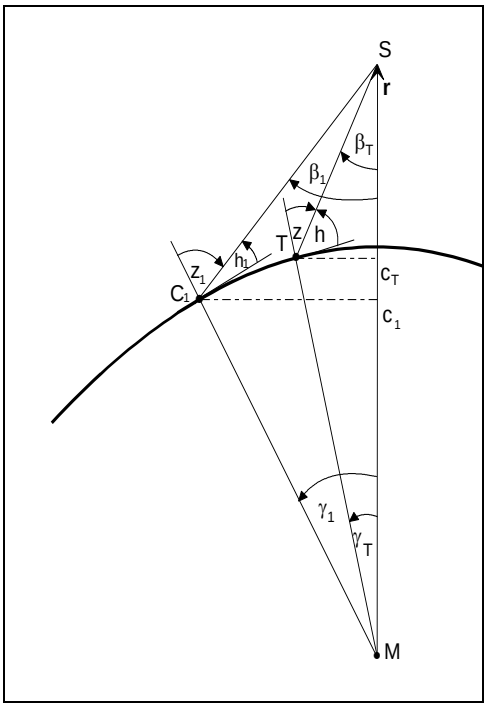

Figure 1: On the computation of the quality of a local coverage: S satellite position, β (off-) nadir angle, *h* elevation, *z* zenith distance, γ central angle (related the Earth centre M), T target point (picture element), C_1 boundary point of observational interval to be covered by the cross scanning sensor

In the frame of a contact time analysis an optimal contact will be defined as the access of a sensor on the Earth's surface (like a ground station antenna) to a sensor onboard a satellite. This geometry corresponds to a maximum elevation of the satellite as seen in the target point. This can be achieved with sufficient accuracy and reliability. The point will be marked in the local diagram as far as it fulfils the observational conditions.

The abscissa of the local diagram corresponds to one day, the resolution for one point will be 12 minutes. However each contact will be accurately grasped (by selectable time steps, usually period/200), so this resolution will be sufficient for long-term investigations. Usually a diagram covers the observability for one month. The duration of a single contact will not be demonstrated in the local coverage diagram because short-term investigation will be treated using other tools such as contact time lists, visibility diagrams etc..
However the quality of a contact will be marked by a characterizing number *K*. This number is based on the elevation *h* of the satellite as seen in the target point. It can be calculated by the condition ('int' means the integer part of the expression in the brackets) K:=int(h/10)+1.
Therefore the interval $0° \le h < 10°$ corresponds to K = 1,

$10° \le h < 20°$ corresponds to K =2, …,

$80° \le h \le 90°$ corresponds to K =9.

There is no uniform use of the designation of the term „incidence angle" in technical applications. Sometimes as incidence angle the elevation *h* will be used, sometimes the zenith distance $z = 90° - h$, which in some cases of satellite orbit analysis will also be called "incidence angle" (cf. 1). This will be used especially for satellites with a SAR (Synthetic Aperture Radar), observing with microwaves. The restrictions for the observability conditions of a cross scanning sensor are limited by the selection either of a minimum elevation h_1 or the corresponding zenith distance $z_1 = 90° - h$, of the nadir angle β_1 or the corresponding central angle γ_1, or by the

corresponding swath width W_1. The observation should be possible on both sides of the satellite path or limited to a small coverage band (e.g. cf. figure 2).

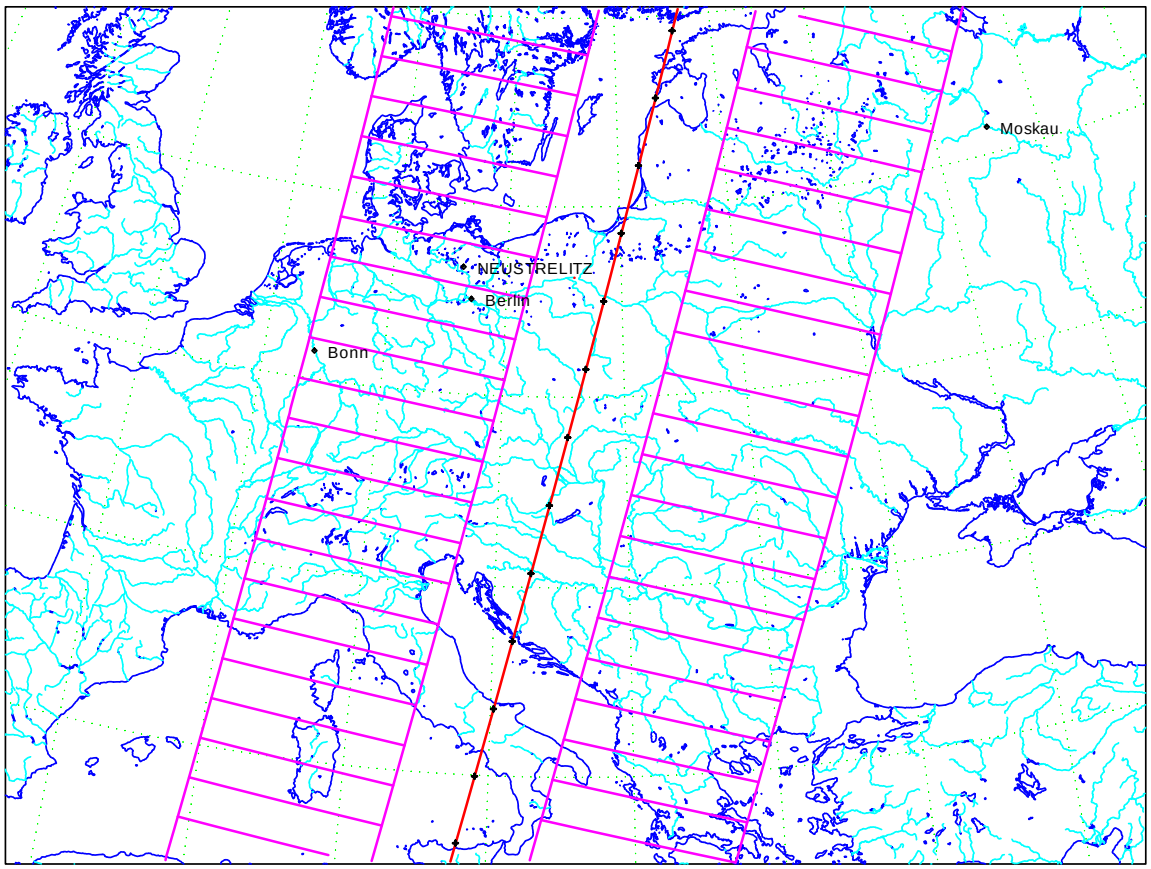

Figure 2: Possible coverage region of an onboard sensor on both sides of a satellite ground track. The free region in the middle part of the coverage region corresponds to an off nadir angle of less than 20°.

2. Classification of Satellites Orbit Families

2.1 Coverage Pattern of Any Earth Observation Satellite

As a first example, the observability condition of a satellite moving on a circular orbit with semimajor axis a = 7278 km (averaged height H = 900 km) and inclination i = 80° will be investigated. The observation will be performed using an optical scanner onboard the satellite on both sides of the satellite path restricted by a minimum elevation of 40° ("incidence angle"). The ground station Reykjavik $\lambda = 338°12'.5, \varphi = 64°8'.9$ will be selected as reference target point.

Figure 3 shows course and quality of the local coverage for one month. The diagram shows 2 – 4 coverages per day. There are frequent near zenith distant passes (h>80°). The daily drift of the passes towards morning hours corresponding to an orbit drift towards west will be recognised. In Figure 2 the diagram as in the classical representation is shown. The corresponding presentation in the new form, using circles and colours, is shown in Figure 3.

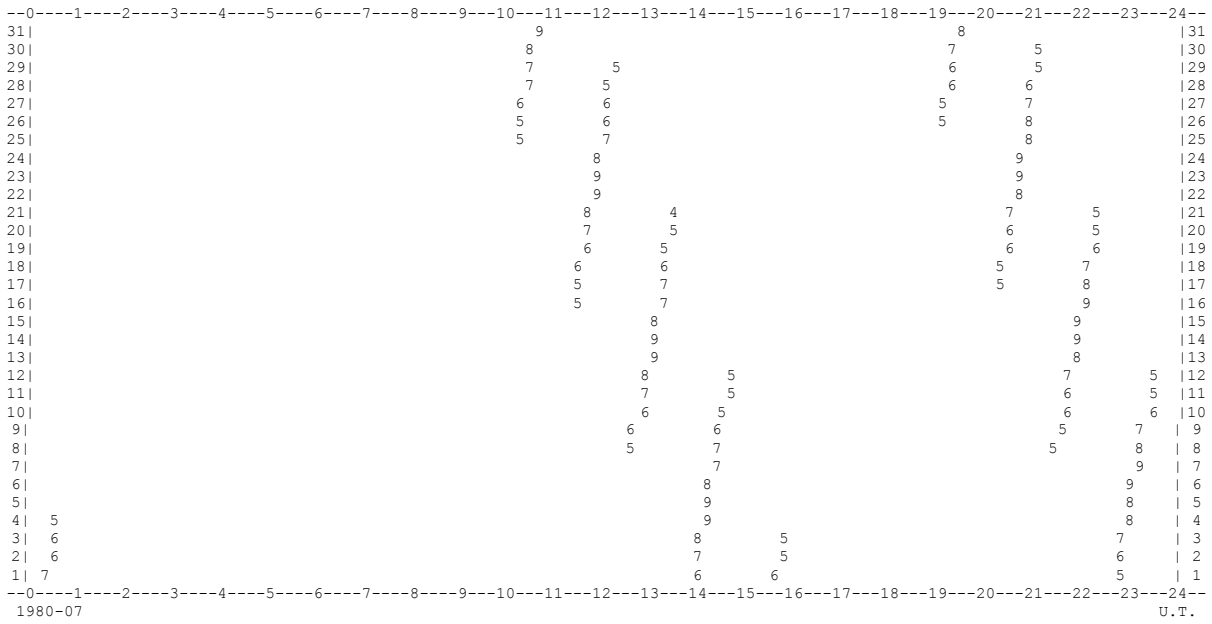

Figure 2: Local coverage diagram for a satellite with cross scanning optical sensor, satellite orbit: a = 7278 km (H= 900 km), e = 0.0, i = 80°, observability condition: elevation h > 40°, target: Reykjavik

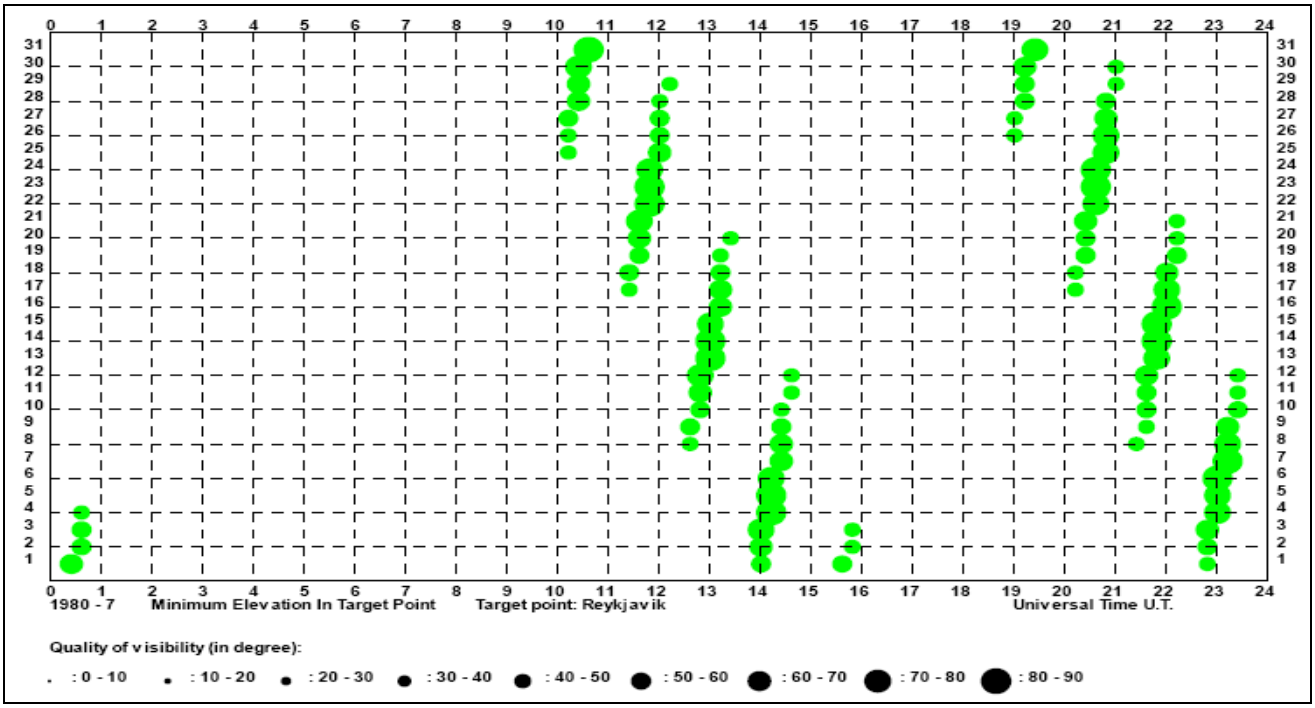

Figure 3: Same issue as in Figure 2 however using the new plot representation

2.2 Coverage Pattern for Satellites with High Daily Drift of Orbital Plane

Observability of the circular orbit H = 450 km, i=53° as observed in ground station Weilheim-Lichtenau under the minimum elevation restriction h=10°. About 5-6 contacts per day will be expected (cf. Figure 4). As a consequence of the inclination of the orbit a maximum drift of the orbital plane towards west by about 6°/day can easily be observed in the diagram.

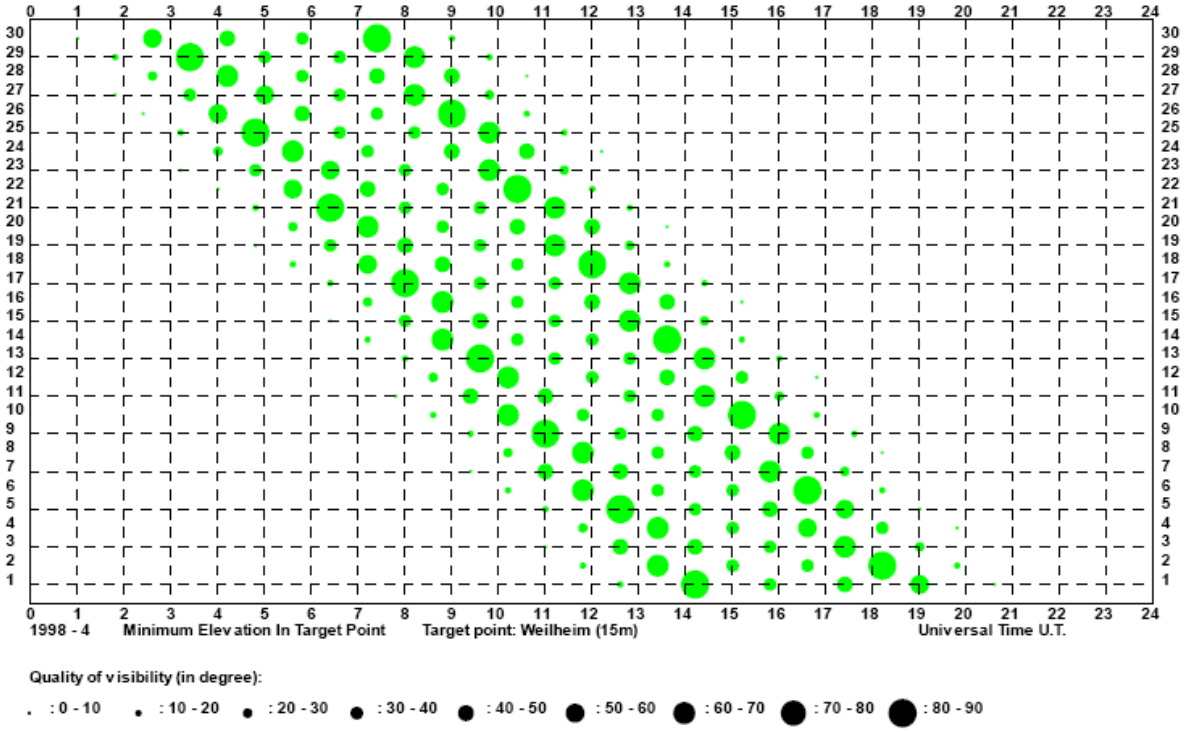

Figure 4: Local coverage diagram for the maximum visibilities of the satellite on the orbit a=6798 km (H= 420 km), e = 0.0, i = 53°, condition of observability: $h \geq 10°$, ground station: Weilheim-Lichtenau (Bavaria)

2.3 Naked Eye Observation of a Satellite as seen from Ground

The international space station (ISS) Station (a = 6732 km, H = 355 km, e = 0.00035, i = 51°.64) will be observed in Munich $\lambda = 11°36'.5, \varphi = 48°8'.8$ for one month. A naked eye observability will be possible, if the satellite will be illuminated by the Sun whereas the observer on the Earth's surface is still (or already) in the dusk, i.e. at times before Sun rising or after Sun setting. The diagram (Figure 5) shows the observability with elevations $h \geq 20°$. A fast drift of the orbital plane towards west can be seen in the diagram. This will be caused by the secular drift of the right ascension of the ascending node by $\dot{\Omega}_s = -5°.11/d$. A consequence will be the rapid change of the Observability of the station from day to day. Observability of the station will occur on evening or in morning hours only. Because of the drift from time to time no observability will be possible. Sometimes but very seldom two observations per day will be possible. However in summer (May – July in the northern hemisphere) 5-6 observations with naked eye can be expected (this can be shown by the local diagram as computed for the months May – July). Excellent Observability with elevations h≥70° is possible about every 3 – 4 days.

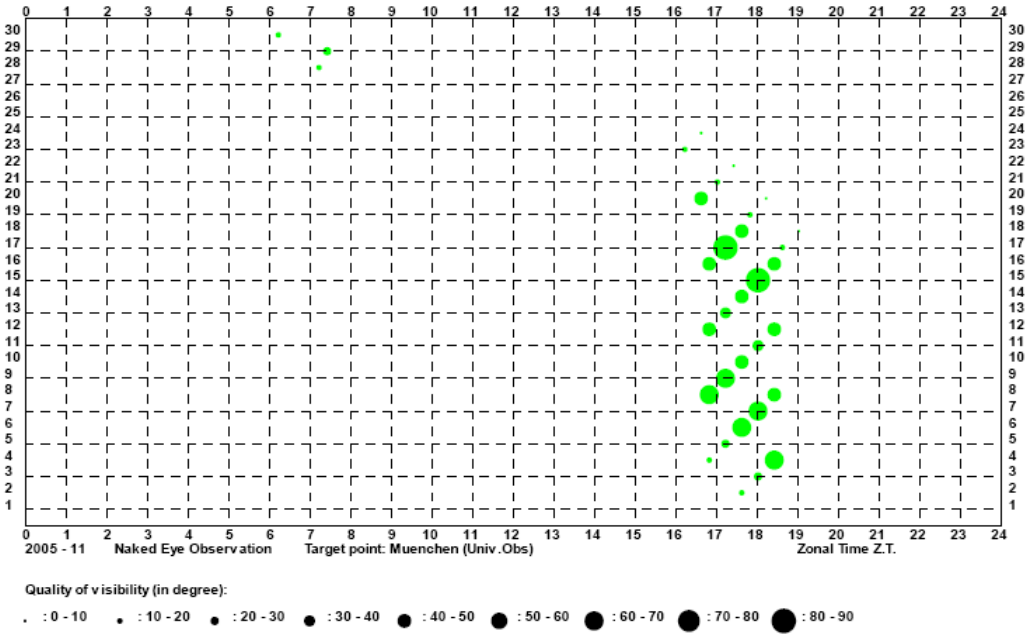

Figure 5: The naked eye observability of the international space station in Munich during the month November 2005. Time in central European time (MEZ ⇔ Z.T. = zonal time)

2.4 Coverage Pattern for Repetitive Satellite Orbit

A satellite orbit with repetitive ground path ("reproducible orbit") shows a remarkable regular coverage pattern in a local coverage diagram.

Figure 6 presents an orbit reproducible after 2 periods of the node (about 2 days but not exactly) and 27 draconic (crossing node related, in English literature usually called "nodal") periods. An onboard optical scanning sensor is able to observe with a maximum nadir angle $\beta \leq 40°$. The diagram presents as characterizing number the elevation as seen from Munich taken as target picture element. The reproducibility of the orbit can clearly be seen in the diagram by the regular repetition of the observability after about 2 days. Because of non-sunsynchronity of this orbit the observation time drifts towards morning times i.e. towards west.

2.5 Coverage Pattern for a Non-Repetitive Sunsynchronous Satellite Orbit

A sun-synchronous orbit will be characterized by an in time stabilized observation bloc. It will not drift in time with respect to the fictive mean Sun (this is defined by projection of the true Sun onto the equatorial plane and by a uniform motion along the equator). Figure 7 shows the local coverage diagram of a circular sun-synchronous orbit (a=7000 km, i=97°.897). The ground station Neustrelitz $(\lambda = 13°4'.1, \varphi = 53°19'.8)$ will be covered as target picture element. The observability condition should be the elevation of satellite h≥20°.

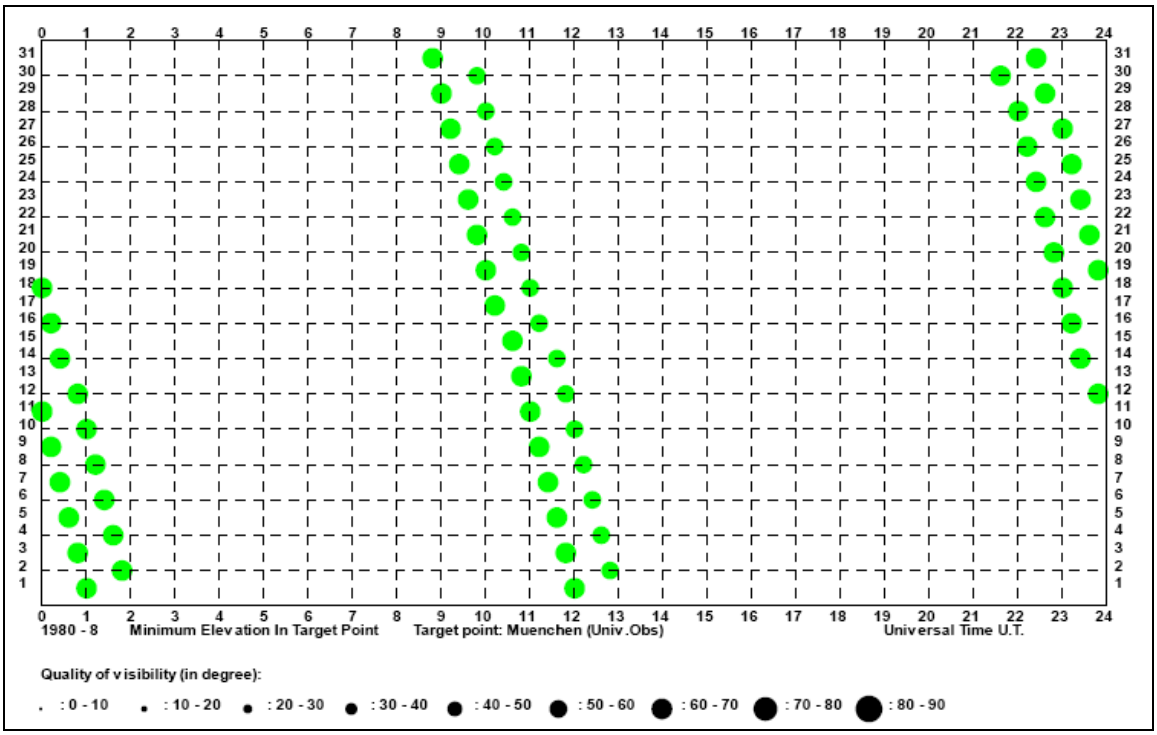

Figure 6: Locale coverage diagram for the circular orbit with 2:27 ground track reproducibility and inclination *i*=83°. Observation of a target picture element in Munich by (off -) nadir angle β=40°

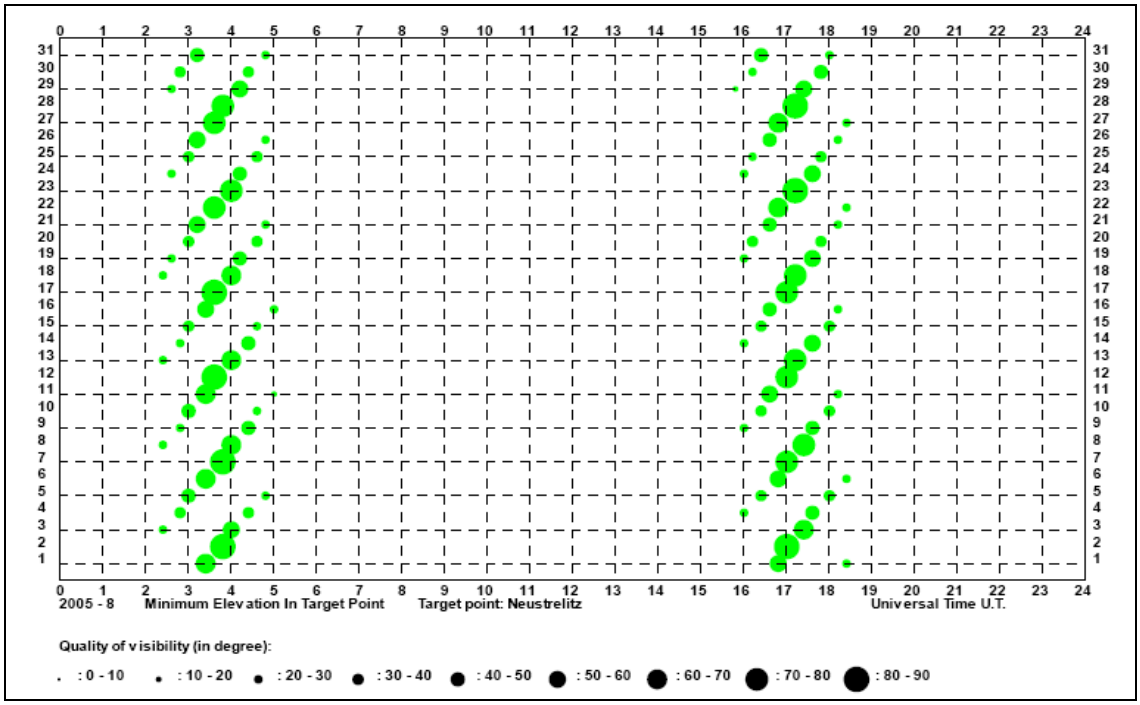

Figure 7: Local coverage diagram for the non-reproducible circular sun-synchronous orbit with semimajor *a*=7000 km and inclination *i*=97°.897. Coverage of a picture element in Neustrelitz by the minimum elevation *h*=20°.

The diagram shows a casual reproducibility after 5 days. However the computation presents an exact reproducibility of 77 days and 1140 draconic periods, corresponding to a subcycle of 5 days and 74 draconic periods. It may be seen that the whole observational bloc is stabile with respect to long-term observations. It cannot be seen from the diagram that the satellite will be on the day in the ascending pass (from south to north) and in the night in descending pass (from north to south). This fact has to be evaluated from the computation and added to the information of the diagram.

2.6 Coverage Pattern for a Repetitive Sunsynchronous Satellite Orbit, 1st Example

A remote sensing satellite with 3:44 reproducible sunsynchronous orbit (a = 7044 km, e = 0.0, i = 98°.073) . The local coverage diagram in figure 8 shows the coverage for an onboard SAR sensor with zenith distance restriction 60°>z>20° left to orbit, i.e. for a local motion related azimuth $A_T = 270°$. The 3 day reproducibility will clearly be recognised in the diagram as well as the time stability as a consequence of sunsynchronity. As consequence of sunsynchronity each pass over the target point will take at the same time and as a consequence of the track reproducibility the observability condition will (after the 3 days repetition pattern) always identical. In the diagram the zenith distance z is selected as characteristic condition for the estimation of the coverage quality. As seen in the diagram (Figure 8) in three days only three coverages will fulfil the condition where 2 coverages occur at one day, one coverage at another day, whereas no coverage takes place at the third day.

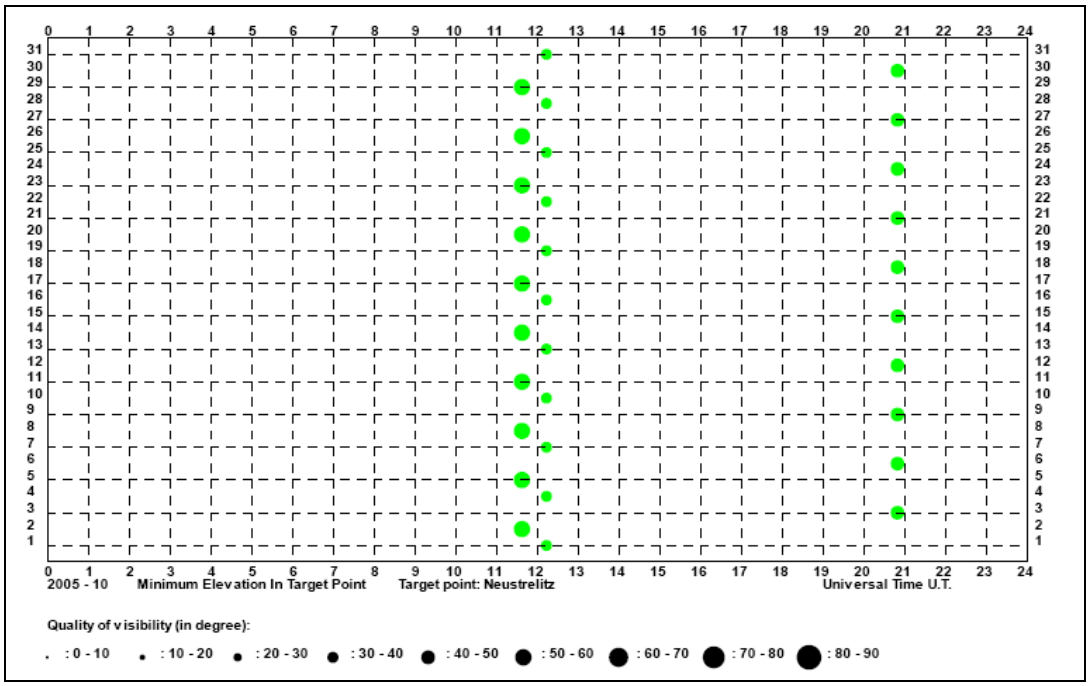

Figure 8: Local coverage diagram for the circular 3:44 reproducible sunsynchronous orbit (semimajor axis a=7044 km, inclination i=98°.073). A coverage band left to the motion direction covers a picture element within the zenith distance interval 60°>z>20°. The diagram shows the coverage for Neustrelitz ground station.

2.7 Coverage Pattern for a Repetitive Sunsynchronous Satellite Orbit, 2nd Example

In addition to Figure 8 the local coverage diagram in Figure 9 shows the coverage of the same target point as seen from the same satellite but for an observation right to direction of motion, i.e. for the satellite centred motion related local Azimuth $A_T = 90°$. As in the previous case the coverage band will be limited by the zenith angle interval 60°>*z*>20°. The coverage at noon all three days will take place with the zenith distance of about 40° during an ascending pass (south to north) of the satellite's orbit. The other 2 possible coverages take place in the night during the descending pass of the satellite, one pass allowing an observation at the boundary zenith distance of about 60°.

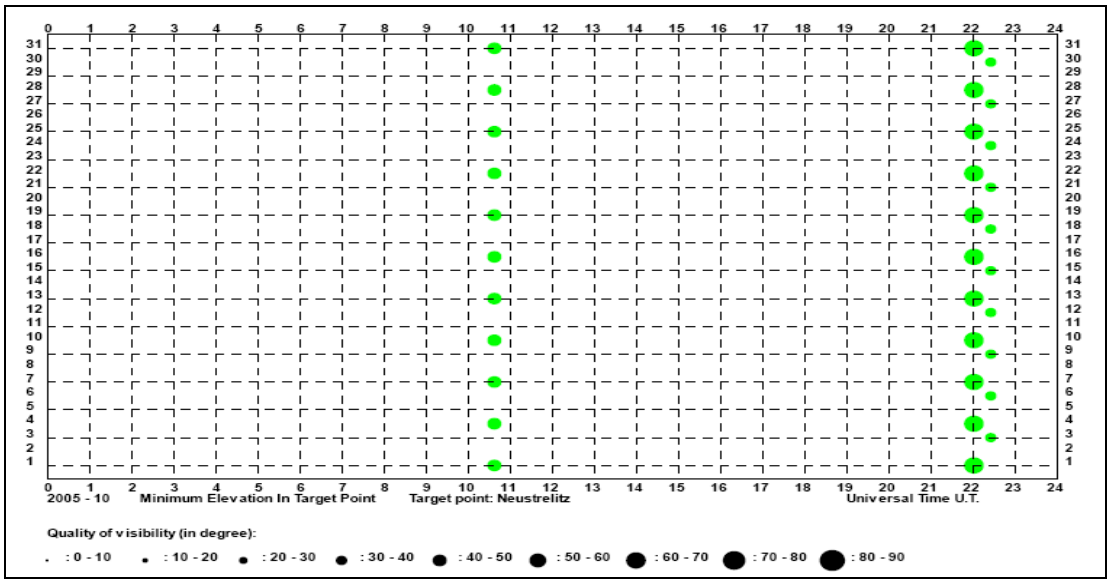

Figure 9: Local coverage diagram for the circular 3:44 reproducible sunsynchronous orbit (semimajor axis a=7044 km, inclination *i*=98°.073) as shown in Figure 8. However in this case a coverage band right to the motion direction is selected to cover a picture element within the zenith distance interval 60°>z>20°. The diagram shows the coverage for Neustrelitz ground station.

2.8 Coverage Pattern for a Repetitive Sunsynchronous Satellite Orbit, Coverage on both Sides of Orbit

In addition to the two previous investigations in Figure 10 the combined observation left and right to the satellite path is demonstrated. This figure shows a combination of the two previous figures. Again the reproducibility of the orbit as well as its sunsynchronity shows an impressive and clear characterisation of such an orbit.

2.9 Coverage Pattern for a Repetitive Sunsynchronous Satellite Orbit, inclusive Orbit Decay due to Air Drag

The same orbit as in the three last figures is selected, however orbit decay due to air drag is assumed as consequence of no orbit keeping manoeuvres. In order to demonstrate the influence of the air drag an unusual air drag is assumed causing a secular decrease of the semimajor axis by

$\dot{a}_s = -0.816 \cdot 10^{-6}\, km/\ s \cong -7\, m/\ d \cong -25.75\, km/\ a.$ This effect will cause a long-term effacement of the ideal picture demonstrated in the previous examples.

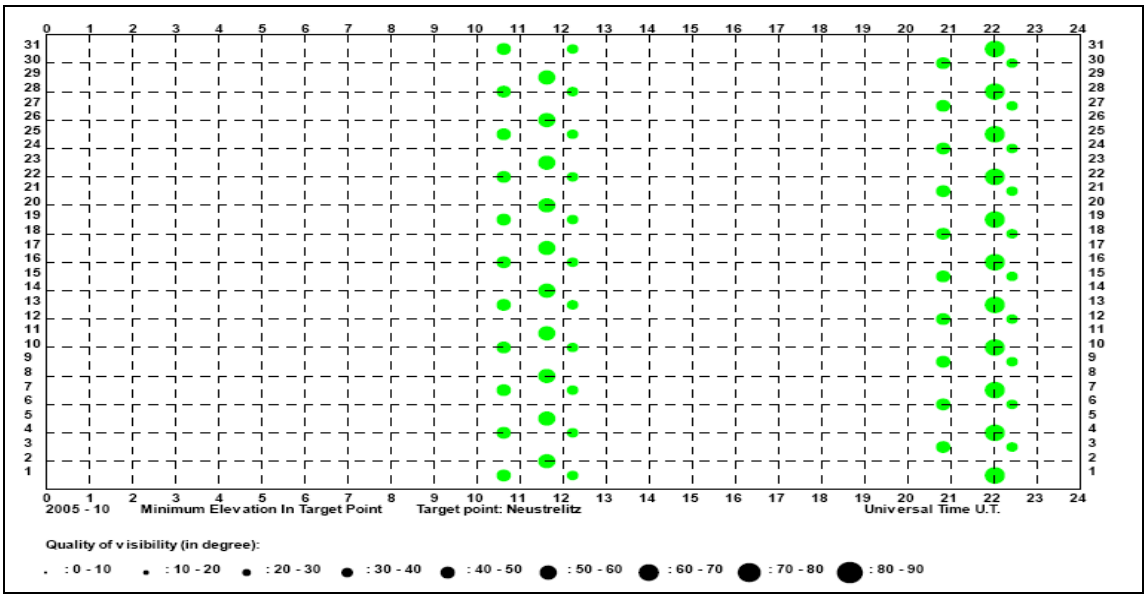

Figure 10: Local coverage diagram for the same orbit as in Figure 8 and Figure 9. In this figure the observability to both sides of the satellite path as a combination of the coverages shown in figures 8 and 9 is demonstrated.

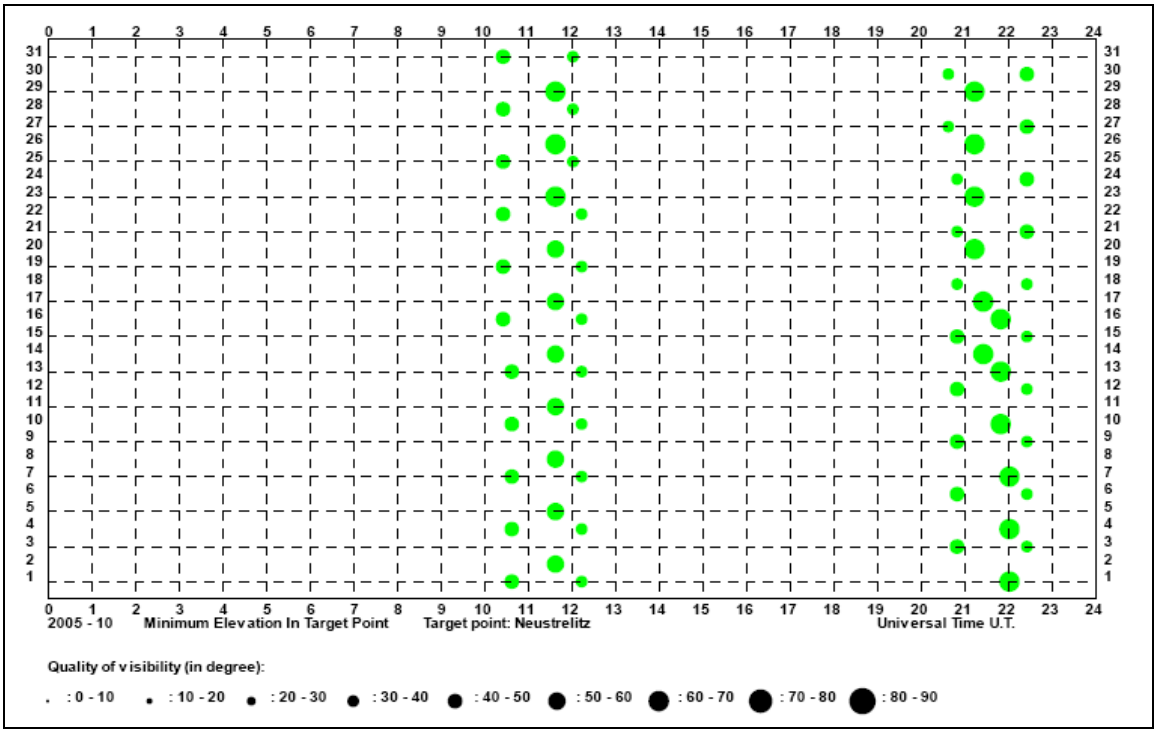

Figure 11: Local coverage diagram for the circular 3:44 reproducible sunsynchronous orbit (semimajor axis a=7044 km, inclination *i*=98°.073) as shown in Figure 8-Figure 10. A coverage band right to the motion direction is selected to cover a picture element within the zenith distance interval 60°>z>20°. The diagram shows the coverage for Neustrelitz ground station. However in this case no orbit maintenance is assumed so that the air drag will cause slow orbit decay

A consequence will be a gradual deviation of the reproducibility and a small shift in time losing the sunsynchronity. This figure (Figure 11) demonstrates the necessity to undertake orbit keeping manoeuvres from time to time. The time interval between two consecutive orbit manoeuvres depends from the solar activity which could be demonstrated in two different local coverage diagrams with respect to different dates within a solar cycle.

2.10 Coverage Pattern for Satellite Orbits with repetition in time due to time shift

The mean solar shift of the ascending node per mean draconic period[4]

$$\overline{\Delta\tau_\Omega} = \dot{\Omega}_s - n_\odot \left[\deg / \overline{P_d} \right]$$

characterizes a special family of satellite orbits. Among them the condition $\overline{\Delta\tau_\Omega} = 0° / \overline{P_d}$ characterizes sunsynchronous orbits. As an extension by selection of the mean solar shift of the node $\overline{\Delta\tau_\Omega} \neq 0° / \overline{P_d}$, Keplerian parameters of a satellite orbit might be computed. E.g. If the eccentricity and the inclination will be chosen the semimajor axis of a satellite orbit can be computed[5]. By means of the solar shift of the node a special relation to the time for an orbit family will be selected. This is possible by using the *Saros-Cycle* of astrodynamics[6], preparing a relation between N_S solar synodic and N_d draconic satellite periods:

$$N_S \overline{P_S} = N_d \overline{P_d} \quad \langle N_S, N_d \in \mathsf{N} \quad .$$

The corresponding solar shift of the node will be

$$\overline{\Delta\tau_\Omega} = 360° \left(\frac{N_S}{N_d} - 1 \right) \quad .$$

Using this relation, orbits will be found which are reproducible in time. However the value of the relation N_S / N_d is very small. Satellite orbits fulfilling a Saros-cycle comprise extremely large time intervals, up to some hundred days. Instead, a shift in mean solar time per draconic period according to the relation

$$\Delta T_m = 4 \times \overline{\Delta\tau_\Omega} \left[\min / \overline{P_d} \right]$$

leads to interesting representations of satellite orbit families. This will be demonstrated in the following using some examples. The progress of time shift ΔT versus orbital inclination is presented in figure 13 for circular orbits and for some different orbital heights. It can be seen, that the time shift will occur only in the interval

$$-2.7\,h / \overline{P_d} \; \square \; -160 \min / \overline{P_d} < \Delta T_m < 2 \min / \overline{P_d} \quad .$$

For near Earth satellite orbits the lower limit of this interval will be about $-8 \min / \overline{P_d}$. In extension, the figure shows that a correlation between time shift and inclination will lead to two

[4] [8] section 28.7.2
[5] [8] section 28.7.4.2
[6] [8] section 28.9.1

different solutions. This is a consequence of the correlation between semimajor axis and solar shift of the node[7].

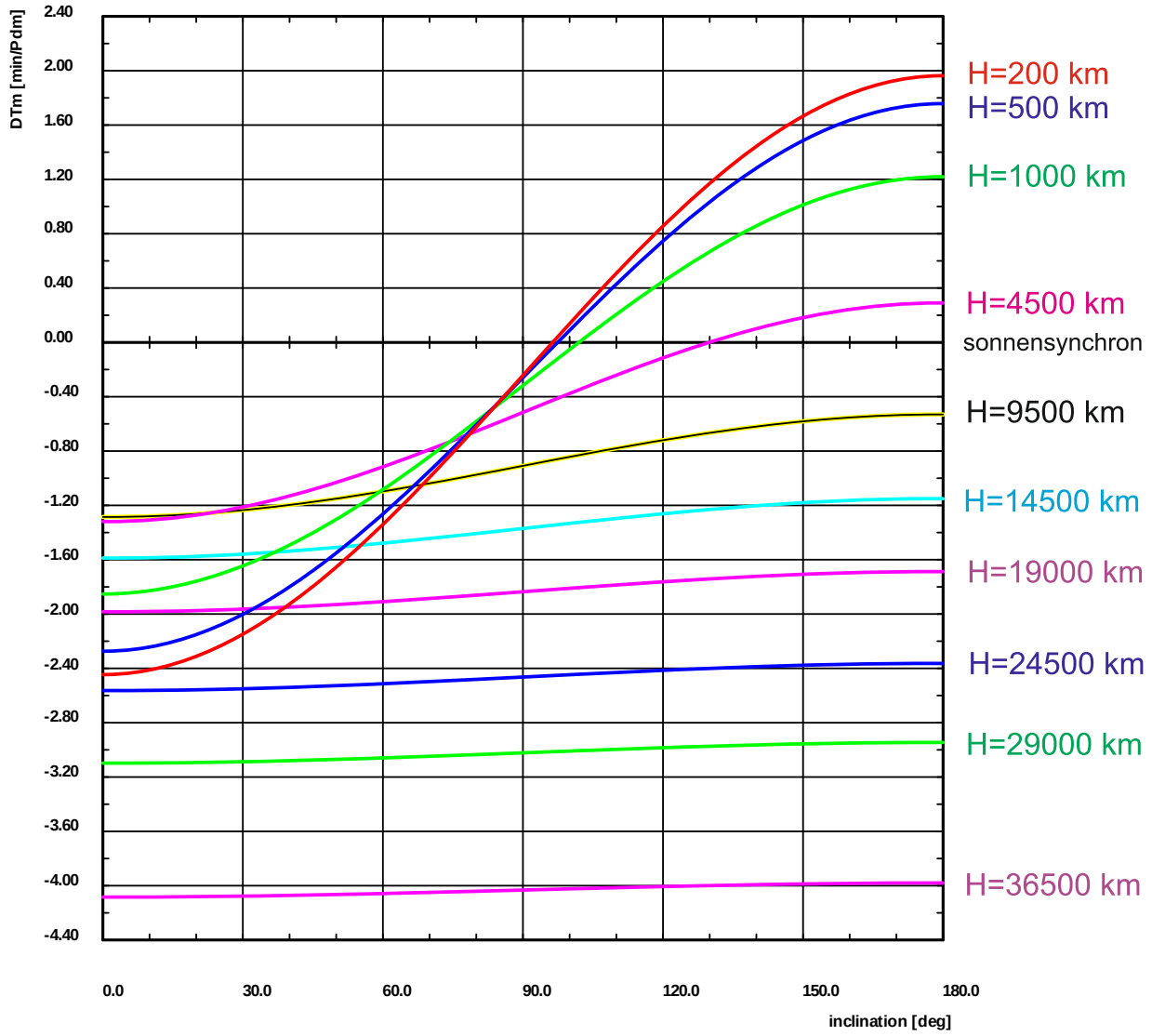

Figure 13: Shift of mean solar time ΔT_m in minutes per one draconic period for all inclinations of circular satellite orbits spread for different satellite heights. A special marc characterizes the sunsynchronous orbit $\Delta T_m = 0.0\,\text{min}$.

Example 1: A circular orbit with inclination 120° and time shift $\Delta T_m = -1.0\,\text{min}/\overline{P_d}$ shall be found. The corresponding solar shift of the node is $\overline{\Delta\tau_\Omega} = -0°.25/\overline{P_d}$. The only possible solution has a semimajor axis of $\bar{a}_0 = 18465.183\,\text{km}$ corresponding to the mean orbital height $H = 12087\,\text{km}$. Figure 14 shows the local coverage diagram in zonal time (MET) for the

[7] As demonstrated in figure 28-25 [8]

German ground station Weilheim. The time shift to earlier local times during one month is indicated by a red line for a selected coverage sequence.◀

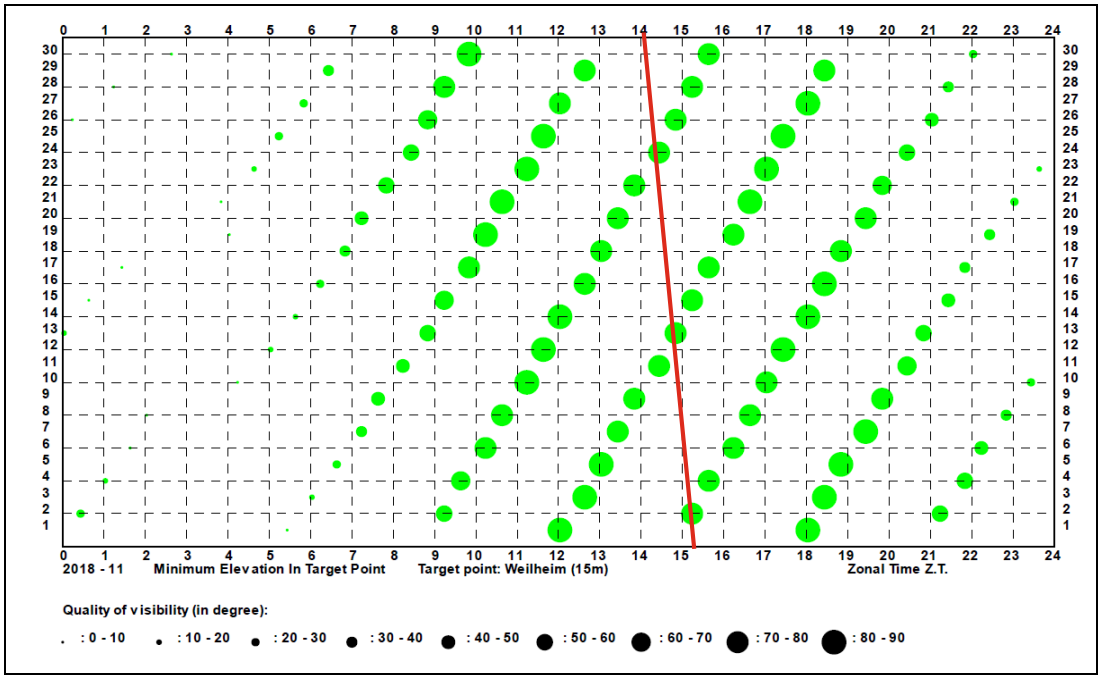

Figure 14: Local coverage diagram for a circular satellite orbit with time shift $\Delta T_m = -1.0\,\text{min}/\,\overline{P_d}$ as observed from German ground station Weilheim: a = 186465 km, e=0.0, i = 120°

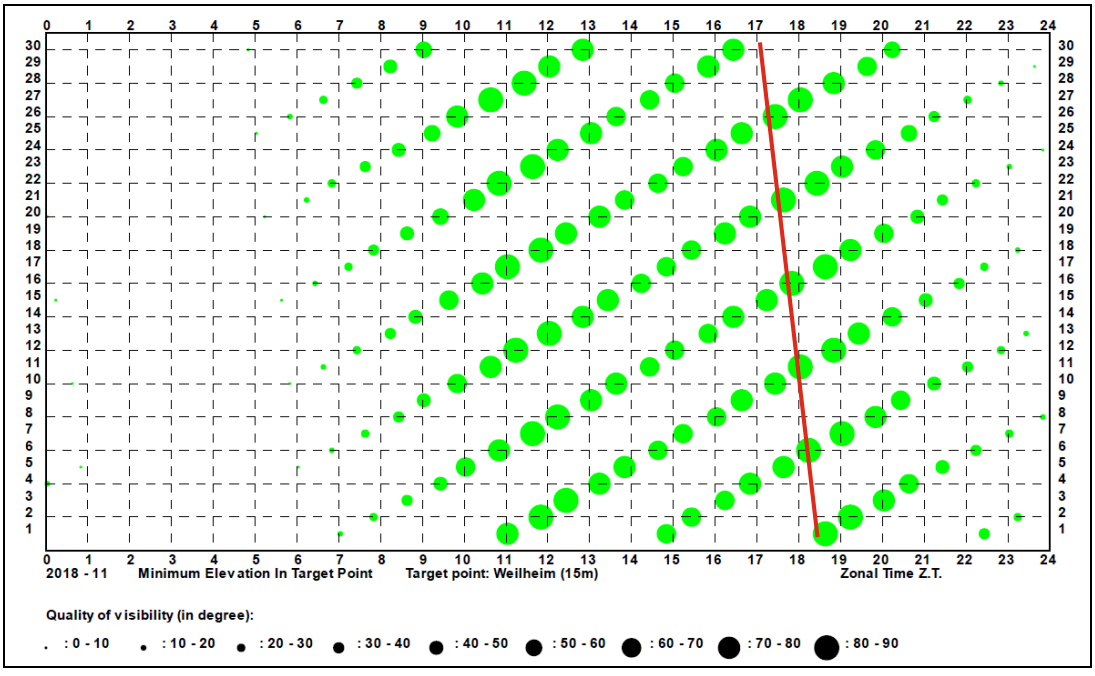

Figure 15: Local coverage diagram for a circular satellite orbit with time shift $\Delta T_m = -0.4\,\text{min}/\,\overline{P_d}$ as observed from German ground station Weilheim: a = 186465 km, e=0.0, i = 120°

Example 2: A circular orbit with inclination 120° and time shift $\Delta T_m = -0.4\,\text{min}/\overline{P_d}$ corresponding to $\overline{\Delta\tau_\Omega} = -0°.1/\overline{P_d}$ shall be found. The only solution has a semimajor axis of $\bar{a}_0 = 13068.458\,\text{km}$ corresponding to the mean orbital height $H = 6690\,\text{km}$. Figure 15 shows the local coverage diagram in zonal time (MET) for the German ground station Weilheim. The time shift to earlier local times during one month is indicated by a red line for a selected coverage sequence.◀

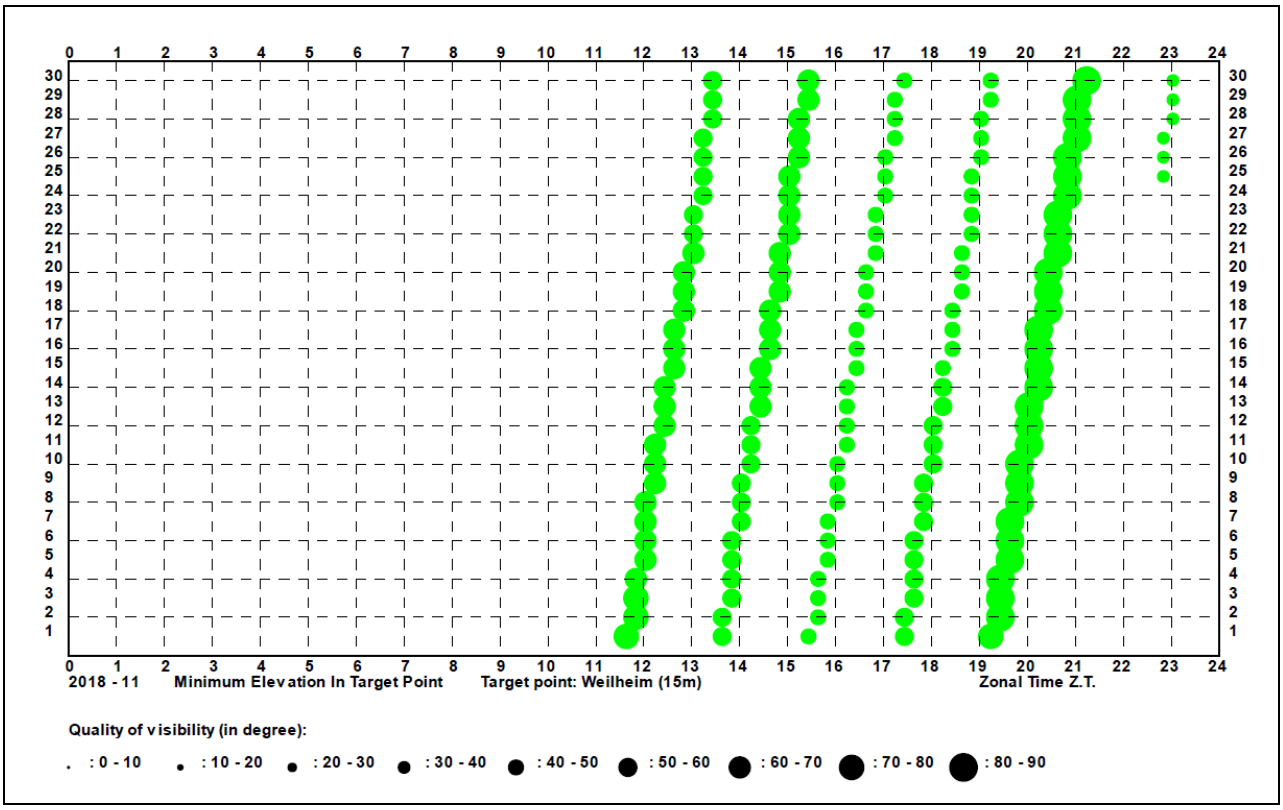

Figure 16: Local coverage diagram for a circular satellite orbit with time shift $\Delta T_m = 0.4\,\text{min}/\overline{P_d}$ as observed from German ground station Weilheim: a = 8072.922 km, e=0.0, i = 120°

Example 3: A circular Earth satellite orbit with inclination 120° and time shift $\Delta T_m = 0.4\,\text{min}/\overline{P_d}$ corresponding to $\overline{\Delta\tau_\Omega} = 0°.1/\overline{P_d}$ shall be found. The only solution has a semimajor axis of $\bar{a}_0 = \text{a} = 8072.922\,\text{km}$ corresponding to the mean orbital height $H = 1694.785362\,\text{km}$. Figure 16 shows the local coverage diagram in zonal time (MET) for the German ground station Weilheim. The time shift to later local times during one month is clearly recognizable by a rectilinear line.◀

3. Examples for an Application of Satellite Control Planning

For satellite control planning a local coverage diagram as shown e.g. in Figure 4 could be a helpful tool. In case of observing different satellites with the same ground antenna and with the same ground station crew the overlapping of different local coverage diagrams each produced for a single satellite may identify rapidly conflict situations.

3.1 Observation of Two Satellites with One Ground Antenna Without Conflict

In Figure 12 the coverage of two satellites (a_1 = 6798.155 km, e_1 = 0.0, i_1 = 53°, $\Omega_1 = \omega_1 = M_{01}$ = 0°; a_2 = 6798.155 km, e_2 = 0.0, i_2 = 97°, $\Omega_2 = \omega_2 = M_{02}$ = 0°) will be compared with respect to the ground station in Weilheim. An overlapping of the two local coverage diagrams will allow a survey of conflict situations. In this case even a penetration of the two coverage regions will not cause any conflict situation with respect to the 12 minute resolution of the plot.

3.2 Observation of Two Satellites with One Ground Antenna Including Conflict Situations

The example presented in Figure 13 shows the overlapping of two satellites (a_1 = 6798.155 km, e_1 = 0.0, i_1 = 53°, $\Omega_1 = \omega_1 = M_{01}$ = 0°; a_2 = 6798.155 km, e_2 = 0.0, i_2 = 45°, $\Omega_2 = \omega_2 = M_{02}$ = 0°) with slightly different inclination. At begin of observation due to identical epoch dates at totally overlapping producing a conflict situation will appear. However the relative drift of the two orbits will cause a relaxation of the conflict situation already after about 12 days.

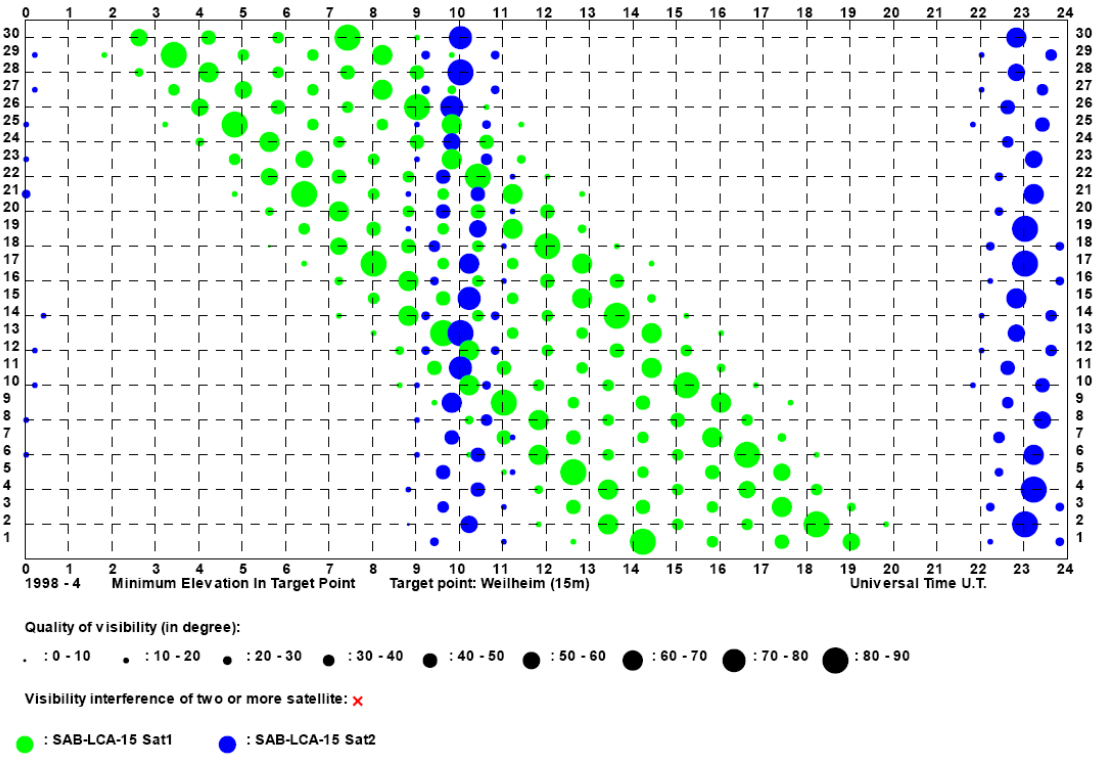

Figure 12: Observation of two different satellites by the same ground station antenna without conflict situations

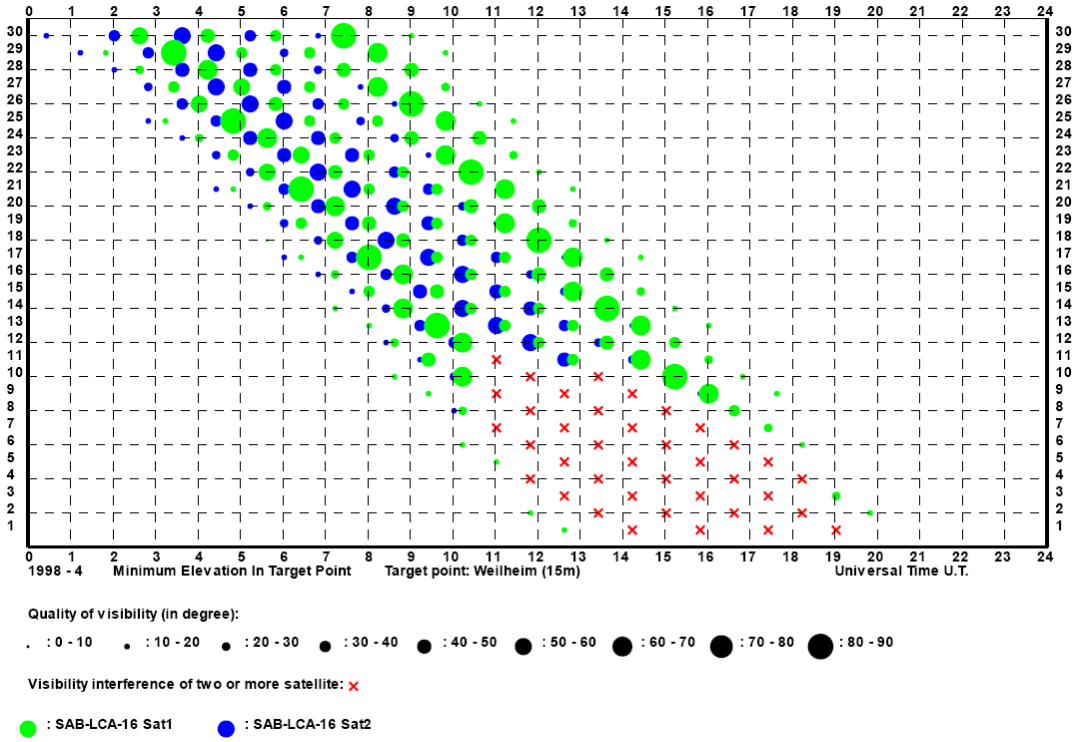

Figure 13 Observation of two different satellites by the same ground station antenna demonstrating conflict situations. The conflicts are characterized by the "x" sign.

4. Application for Satellite Constellation Investigations

4.1 Satellite Constellation with four Integer Orbits

Selected will be a family of four 1:15 integer orbits covering the whole Earth on one single day. The satellites will move in the same inertial orbital plane, each a fourth of the draconic period behind the other. Therefore a global coverage of the whole Earth's surface during one day will be achieved (Figure 14). This orbit behaviour will be reflected in the coverage of one ground station as shown in Figure 15: Due to the sunsynchronity of the orbits, each satellite will pass over this station at the same mean day time, each of them with the identical quality, i.e. under the identical maximum elevation and pass behaviour.

4.2 Satellite Constellation with Three Sunsynchronous Orbits in Different Orbital Planes

The example shown in Figure 16 presents the coverage behaviour of three satellites in different orbital planes ($a_1 = a_2 = a_3 = 6868.100$ km, $e_1 = e_2 = e_3 = 0.0$, $i_1 = i_2 = i_3 = 98°.15$, $\Omega_1 = 0°$, $\Omega_2 = 63°.6$, $\Omega_3 = 129°$, $\omega_1 = \omega_2 = \omega_3 = 0°$, $M_{01} = 0°$, $M_{02} = 35°.5$, $M_{03} = 0°$). The contact times for all satellites are separate, only a few conflict situations with very low maximum elevation will be expected. However these situations with very bad observability will be neglected.

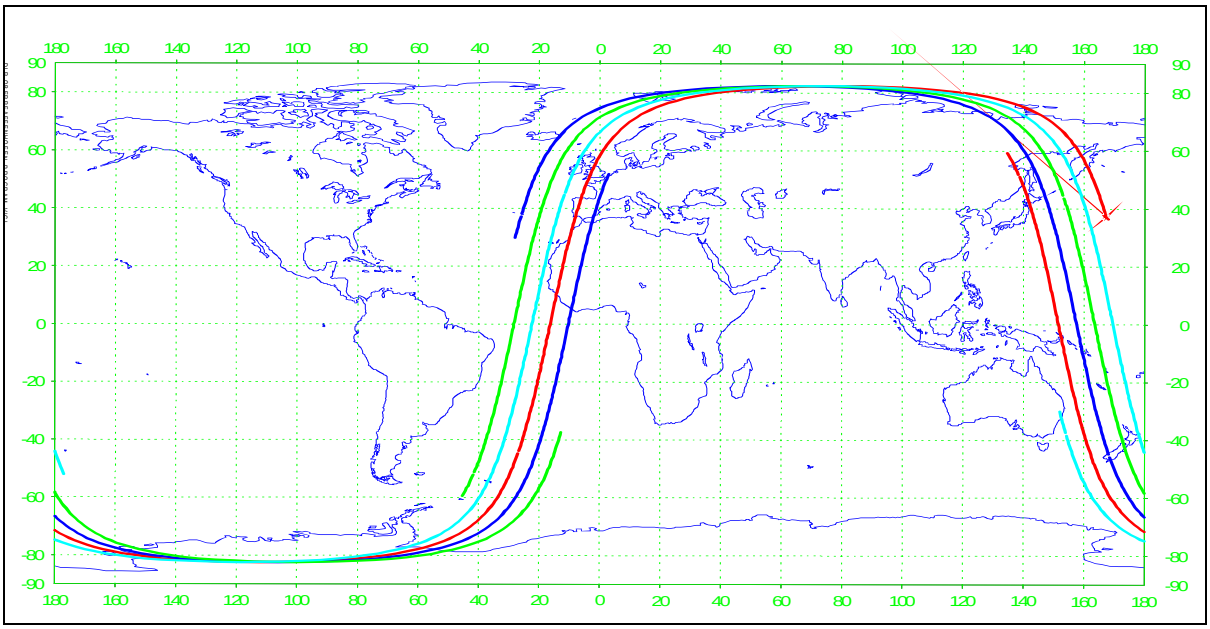

Figure 14: Ground track of the four satellites of the constellation for one period

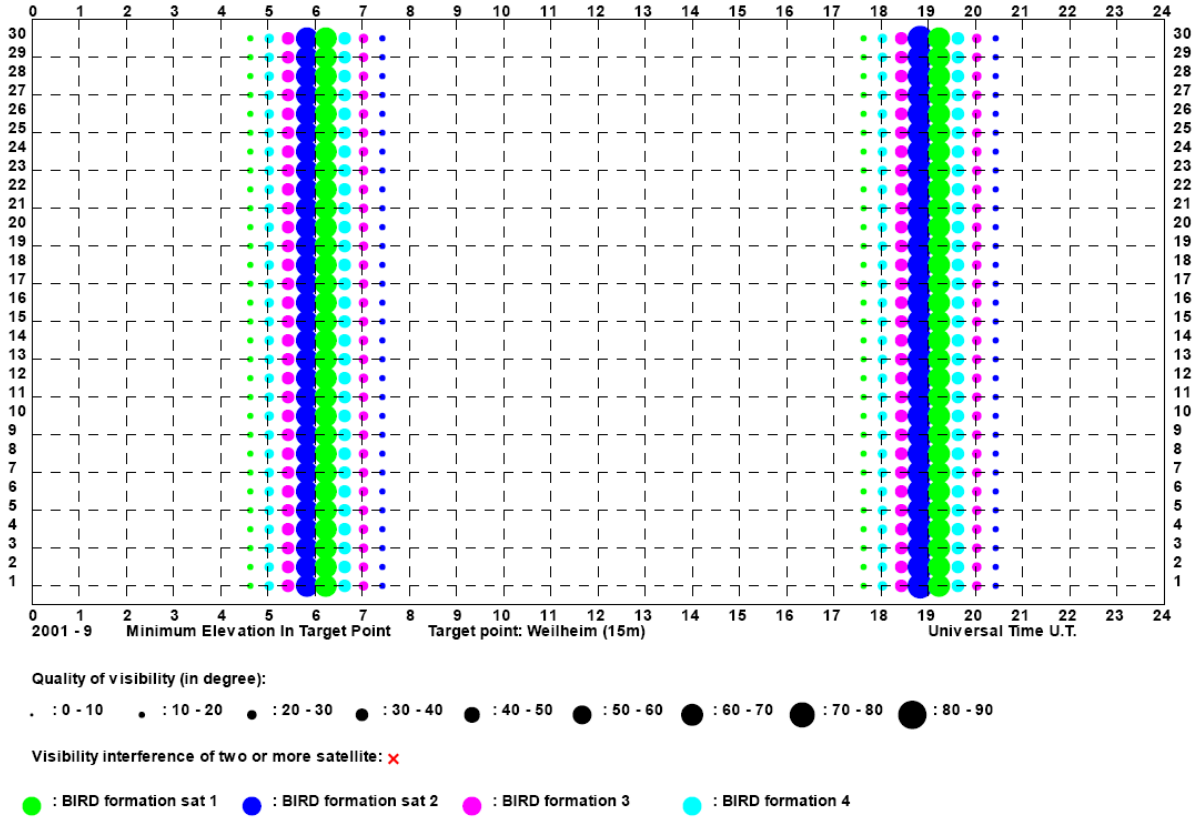

Figure 15: Coverage of four satellite orbits (of the BIRD type, each on a 1:15 integer orbit) of a satellite constellation

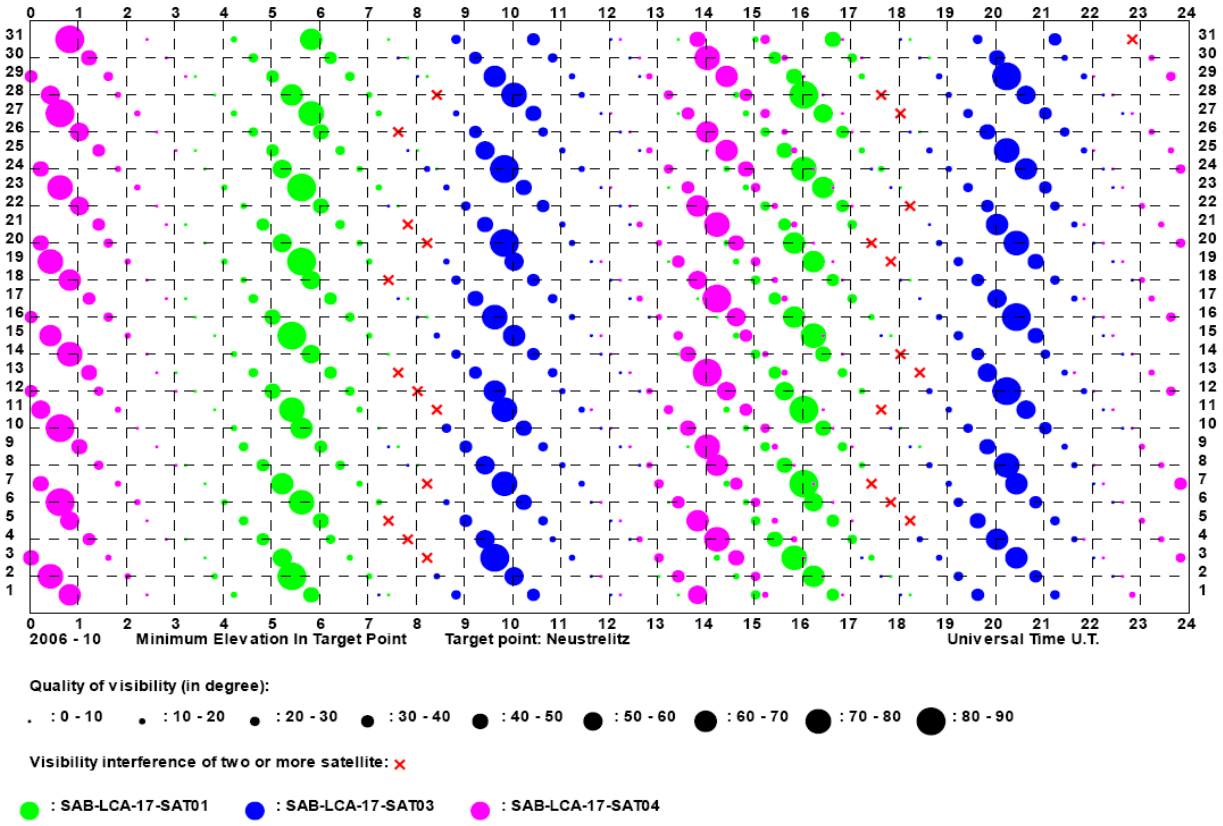

Figure 16: Coverage behaviour of three near circular and near sunsynchronous satellite orbits of a satellite constellation as observed in Neustrelitz ground station

Conclusion

The local coverage diagram will be used for long-term investigations of the coverage behaviour of a certain bore sight point on the Earth's surface. It shows a completely different and therefore typically characterizing pattern for each kind of satellite orbits. Special emphasis can be achieved for investigations of satellite constellations with respect to the coverage of special points of interest for Earth reconnaissance satellite families. Therefore the local coverage diagram is very useful to support long-term mission planning as well as to facilitate the demonstration of satellite orbit developments in the context of educational purposes. The local coverage diagram is able to be an essential auxiliary tool for satellite orbit analysis of near Earth satellite orbits.

Longterm observations of satellite orbits show a characteristic pattern presented by the local coverage diagram. A series of typical diagrams as presented in the present paper and further developed on the basis of these diagrams will allow a fast overview of different Earth satellite families.

Appendix

The theory of local coverage diagrams is independent of a special software tool. The results presented in this paper are obtained with a software module incorporated in the DLR orbit analysis tool VENI, VIDI, VICI. This tool is dedicated to visibility and coverage investigations

including orbit prediction and visualization of geocentric and heliocentric orbits. For these investigations the analytical orbit propagator from *Brouwer-Lyddane-Eckstein* is used [2].

References

[1] CALAMINUS, B. [2007]: 'Entwicklung einer Software zur Erstellung und Auswertung von lokalen Überdeckungsdiagrammen von Satellitenbahnen bezüglich ausgewählter Bodenstationen', Diplomarbeit Hochschule Albstadt-Sigmaringen, März 2007

[2] ECKSTEIN, M. C. [1973/1974]: 'Ein Satellitenbahnmodell ohne Singularitäten', DLR-FB 73-67, 'A Satellite Model without Singularities', ESRO TT-102, Oct. 1974

[3] JOCHIM, E. F [1974] : 'Sichtbarkeitsuntersuchungen für die Satelliten SYMPHONIE A und B'. DFVLR-DF Interner Bericht IB 552 - 74/5

[4] JOCHIM, E. F [1975]: 'SICHDI. Ein Programm für Sichtbarkeitsdiagramme für Satelliten mit großer Halbachse'. Benutzeranweisung. DFVLR-DF Interner Ber. IB 552-75/14

[5] JOCHIM, E. F.; PIETRASS, A. E. [1976]: 'Beobachtungsraster eines vorgegebenen Ortes durch einen Erderkundungssatelliten mit Scan-Sensor'. Beschreibung des Programms SCANSI'. DFVLR-DF, *IB* 552-76/14

[6] JOCHIM, E. F [1979]: 'Visibility Diagrams for Satellite Orbit Analysis'. Manual of the FORTRAN Program VIDI. DFVLR-DF Internal Rep. IB 552-78/11

[7] JOCHIM, E. F [2018]: *Satellitenbewegung, Band V, Bewegung und Beobachtungsgeometrie* (Satellite Motion, Vol. V.: The Connection of Motion and Observational Geometry), ISRN DLR FB 2013-12, ISSN 1434-8454 (second edition, primary issue in 2013). Ch.35

[8] JOCHIM, E. F [2018]: *Satellitenbewegung, Band IV, Bewegungsanalyse* (Satellite Motion, Vol. IV.:Satellite Orbit Analysis), ISRN DLR FB 2018-31, ISSN 1434-8454

[9] NEFF, TH., JOCHIM, E. F., PIETRASS, A., KIRSCHNER, M., CALAMINUS, B. [2008]: 'The Local Coverage Diagram', AIAA-AAS Astrodynamics Conference, Honolulu, Ohau, Hawaii, 2008-August-19, AIAA-2008-6608